24-034

Enhancing Ventilation and Development Planning in Underground Stone Mines: Insights from a CFD-Based Study

Khaled Mohamed
CDC NIOSH, Pittsburgh, PA

Marcia Harris
CDC NIOSH, Pittsburgh, PA

Vasu Gangrade
CDC NIOSH, Pittsburgh, PA

Jim Addis
CDC NIOSH, Pittsburgh, PA

Kumar Vaibhav Raj
CDC NIOSH, Spokane, WA

Snigdha Sarkar
KETIV Technologies, Brea, California

ABSTRACT

The National Institute for Occupational Safety and Health (NIOSH) conducted a ventilation assessment for a recently established underground room-and-pillar stone mine implementing split-mine ventilation. The primary objective was to examine the impact of the length of the in-place stone stoppings on face ventilation efficiency. These stone stoppings serve to separate the intake and exhaust entries and align with the mining direction. To achieve this, computational fluid dynamics (CFD) modeling was utilized. The appropriate turbulence model was selected, and a mesh convergence analysis was conducted for the CFD model. Following that, the CFD model was validated using the conducted ventilation surveys.

Two configurations of in-place stone stoppings, designated as Layout-I and Layout-II, were simulated using the validated CFD models. Layout-I featured a shorter in-place stone stopping, while Layout-II had a longer one. The results obtained from the CFD models demonstrated that the increased length of the in-place stone stopping in Layout-II resulted in a notable enhancement in ventilation efficiency at the advanced faces (last stopping), elevating it from 4% in Layout-I to 8.4% in Layout-II. However, no significant impact of the in-place stopping layouts was observed at other faces. In general, Layout-II exhibited a greater circulation of air at the outby stoppings.

INTRODUCTION

Stone mines produce a wide range of raw material such as basalt, granite, limestone, marble, etc. for the construction industry needed for infrastructure development. As of 2020, there are 4,248 stone mining operations with 110 underground operations in the United States (NMA, 2020).

Underground stone mines come with a unique set of challenges, of which ventilation is often the primary challenge. Ventilation of these mines is challenging because of the large entry sizes leading to low airflow velocities and increased natural ventilation effects (Watkins and Gangrade, 2022). To establish effective ventilation in such mines, it typically necessitates delivering the required air volumes and effective planning and positioning ventilation control equipment, such as auxiliary fans and stoppings (Grau and Krog, 2009).

Throughout the 2000s, NIOSH conducted an extensive research initiative dedicated to investigating ventilation in large-opening mines. This research emphasized a significant ventilation challenge faced by these mines, specifically the effective planning of airflow direction (Grau et al. 2006). Studies assessing the effectiveness of various ventilation stoppings within large-opening stone mines revealed that in-place stone stopping could fulfill the same function as a series of stoppings (Krog et al., 2004). Testing

small changes in ventilation layouts in operating stone mines can be disruptive and time-consuming. Fortunately, in the present times, we have the advantage of computational fluid mechanics capabilities, which have revolutionized the way we assess and improve ventilation systems in these environments. These advanced tools enable us to simulate and model different ventilation configurations, helping mine operators make informed decisions without the need for extensive physical adjustments. This not only saves time and minimizes disruptions but also ensures that ventilation improvements are more efficient and effective, ultimately contributing to a safer and more productive mining operation.

CFD modeling is a powerful tool to analyze and design mine ventilation systems. CFD modeling has found extensive applications across various domains, encompassing the analysis of airflow patterns and the dispersion of particulate matter and gaseous contaminants in diverse mining environments, ranging from underground mines to open-pit operations (Raj et al., 2023; Bhargava et al., 2021; Morla et al., 2021).

Watkins and Gangrade (2022) utilized a combination of on-site measurements and CFD simulations to identify the optimal locations for auxiliary fan placement, aiming to maximize airflow at intersections within the mine entrance. Their CFD analysis, as outlined in their study, showcased that such optimization could yield a substantial increase in ventilation flow rates and reduce air recirculation. These enhancements serve to elevate the overall efficiency of ventilation systems in large-opening stone mines, thereby reducing worker exposure to airborne contaminants (Watkins and Gangrade, 2022).

In a parallel investigation, Gendrue et al. (2023) conducted a field survey within a large-opening stone mine, using the collected survey data as inputs for numerical modeling in a CFD model. This study aimed to assess booster fan airflow distribution. The modeling results underscored the efficacy of the booster fan as a ventilation control mechanism for directing airflow within large-opening mines, with its placement proving to be a critical factor influencing the removal of pollutants by mitigating airflow recirculation.

This study differs from previous research (Watkins, 2022 and Gendrue,2023) in two main ways. First, it provides a more thorough CFD model for ventilating stone mines. Second, it uses CFD methods to gain insights into the effects of long stone stoppings. This research will present a comprehensive three-dimensional CFD model for a large stone mine using the ANSYS-Fluent software. The main goal of this study is to examine how two layouts of in-place stone stoppings affect the efficiency of face ventilation and air recirculation at crosscuts between exhaust and intake entries.

MINE DESCRIPTION AND FIELD SURVEY

In the winter of 2023, NIOSH conducted the first survey of air velocity within an underground limestone mine in Pennsylvania. The primary objectives of this in-mine survey were to establish boundary conditions, optimize mesh size, and identify the most suitable turbulence model for a proposed CFD model. This partner mine employs a standard split ventilation system, utilizing three primary entrances to the mine: two for air intake and one for air return (Figure 1). The intake and return portals are closely positioned and at same elevations. On average, the entry dimensions in the mine measured approximately 9.15 m in height and 15.24 m in width. The mine employed two 1.83-m propeller booster fans (Figure 2d) with each fan capable of delivering a flow rate of 65.18 m^3/s. The fans are operated under a fixed static pressure of 249 Pa. The intake fan was situated in the third open crosscut between the first portal and the second portal entry, inby from the mine entrance (Figure 1). It functioned to introduce external air into the mine and direct it towards the entryways on the right or southwest side of the portals. The exhaust fan was located at the last open crosscut going outby to direct air out through the third cross-cut.

At the time of the ventilation survey, the mine had not yet commenced production activities, and thus, there was no haul truck traffic within the mine. The only operations

Figure 1. Mine layout showing ventilation control and stations of first ventilation survey (S1–S33)

taking place were scaling operations at various working faces. Both mine fans were operational during the ventilation survey. Initially, the curtain in Entry 94 was open, and although efforts were made to close it as effectively as possible, there was still some air leakage (see Figure 2). The survey within the partner mine involved conducting 60-second anemometer traverses. A vane anemometer was attached to the end of a telescoping pole, extending to 4.27 m in length. Researchers were able to reach heights ranging from 4.88 m to 5.49 m within the mine entry when fully extending the telescoping pole. Throughout the mine, measurements were taken and recorded at 33 surveyed stations, as shown in Figure 1. By extending the pole to its maximum length, the vane anemometer was utilized to traverse the "accessible" regions of the mine entry, thereby determining air velocity. To ensure precise velocity measurements, the traverse measurements were repeated until readings consistently agreed within a 10% margin of error. Taking into consideration the entry dimensions and the average velocity measurements obtained, the volumetric airflow rate was subsequently calculated. Additionally, smoke tubes were employed in the mine ventilation surveys to visualize the flow of air including stagnant areas within the underground mine. These surveys documented various airflow patterns, including regions where air stagnation was observed.

In the late spring of 2023, a second ventilation survey was carried out within the partner mine. During this survey, it was noted that there had been some minor alterations to the mine's boundaries since the first survey. The most significant change compared to the initial survey was the mine was in active production, with haul trucks observed entering through the intake-1 portal and exiting through the intake-2 portal. Furthermore, it was observed that the curtain in Entry 94 was close. Another noteworthy change was the adjustment of the intake fan's orientation, which had been redirected away from the adjacent rib toward the inby of Entry 93 to enhance the airflow towards the advanced faces at entries M-59 and M-61. During this survey, air velocity and direction measurements were taken and recorded at 50 survey stations throughout the mine. The data collected during this second survey served two primary purposes: first, to validate the CFD model, and second, to provide input data for CFD models used to study the impact of in-place stone stoppings on ventilation efficiency at working faces.

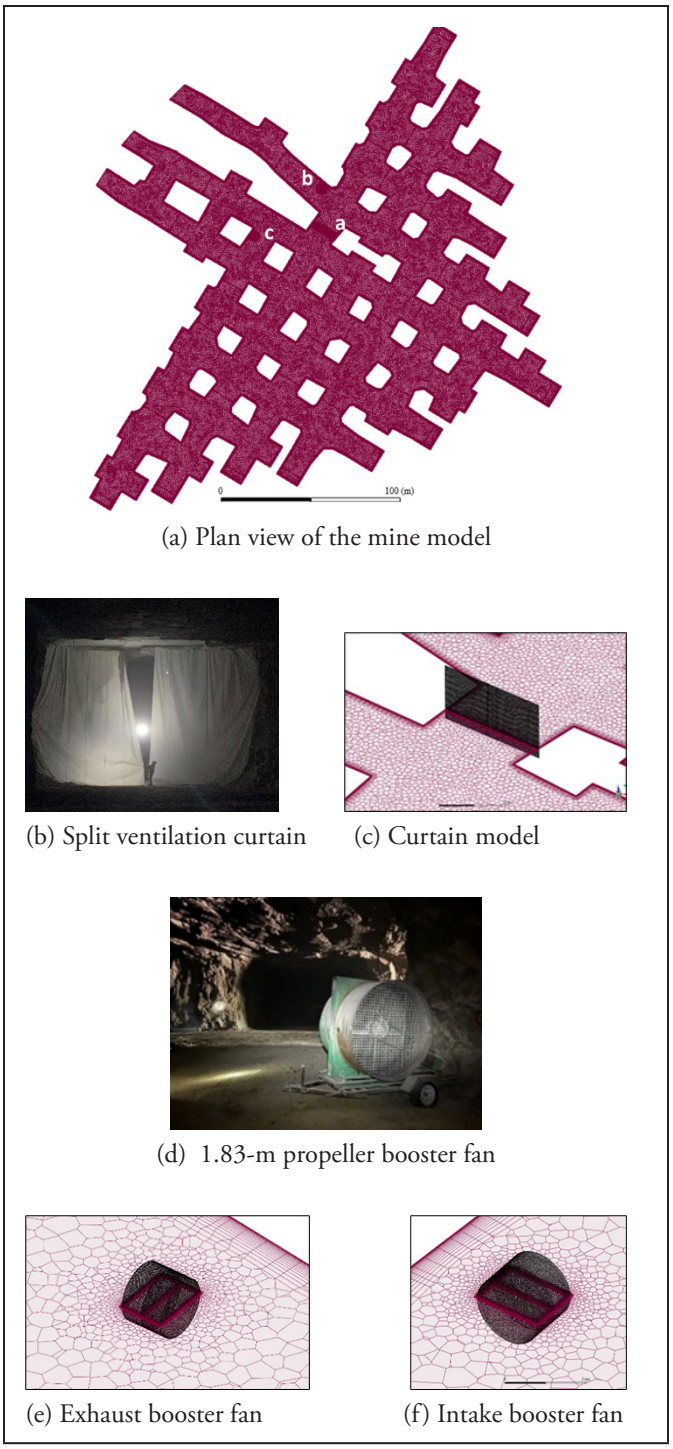

(a) Plan view of the mine model

(b) Split ventilation curtain

(c) Curtain model

(d) 1.83-m propeller booster fan

(e) Exhaust booster fan

(f) Intake booster fan

Figure 2. Planview of CFD model mesh with three-dimensional close-up focus on the curtain and booster fans

CFD MODEL SETUP

The study employed ANSYS-Fluent (ANSYS Inc., 2023), which is commonly utilized by numerous researchers in the field of underground ventilation engineering for investigating various fluid-flow and heat transfer issues. To simulate the airflow within the study mine, a three-dimensional, steady-state, and incompressible solution for the Navier-Stokes equations was employed. ANSYS-Fluent solves these equations in their Reynolds-averaged

Navier-Stokes (RANS) form, considering mass and momentum conservation. The analysis was performed using the k-epsilon turbulence model with scalable wall function. The coupling of momentum and continuity equations for the pressure-velocity interactions was achieved using the coupled scheme.

Because the intake and return portals were being positioned at same elevations and the minimal air resistance posed by large-opening stone mines, it is inferred that the airflow through the intake portals predominantly depends on the size and capacity of intake booster fans and its operating condition. Consequently, a pressure inlet boundary condition was assumed for the model's inlets, while a pressure outlet condition was defined for the model's outlet. The 1.83-meter booster fans (Figure 2d) within the model were simulated using fan boundary conditions with constant pressure gradients of 249 Pa. The fan casings, extending 1.37 m in length, were defined as smooth walls with no-slip conditions. The left and right sections of the curtain were identified as internal smooth walls with no-slip conditions, while a gap between the wall sections (approximately 1.5 m) was modeled as an internal surface (Figure 2c). The external walls of the model were defined as rough walls with no-slip conditions, assuming a wall roughness of 0.04 m (Gendrue et al., 2023). Furthermore, gravity was considered in the Z-direction, and the model was solved to achieve a convergence level of 1×10^{-3} for velocity components (X, Y, Z), mass flow, and turbulent energy. Typically, the models successfully converged within the range of 200–300 iterations. However, the solution process was continued up to a total of 1,000 iterations to ensure that the monitored velocities at the designated monitoring stations marked as S1-S33 (see Figure 1) and the fan velocities had reached their steady-state conditions.

For airflows within large-opening stone mines, where wall-bounded effects are of lesser concern and separation primarily arises from approaching stone pillars, the adoption of a k-epsilon-based wall function approach is believed to be suitable. In employing wall function models, it is advisable to maintain a y-plus value greater than 30 to mitigate inaccuracies in modeling the buffer layer and laminar sublayer. The CFD simulation of airflow within such mines encompasses a broad spectrum of air velocity scales, with air velocities at booster fans falling between 15–20 m/s while other locations exhibit fractions of m/s. Consequently, the model grid and near-wall refinement incorporate varying levels of y-plus, potentially placing certain areas within the viscous and buffer layers. Hence, the recommendation is to employ a scalable wall function in such scenarios. In Ansys Fluent, this specialized wall function effectively relocates the near-wall mesh to a y* value of 11.225 where y* is another unit for dimensionless distance from the wall similar to y-plus. This y* value of 11.225 marks the transition into the log-law region. It is important to acknowledge that, for grids designed with a y* greater than 11.225, the scalable wall function will yield results consistent with those obtained using the standard wall function.

When using wall function models, a minimum of 10 cells is needed to accurately capture a boundary layer, but values of 20 are more desirable. Therefore, the boundary layer built at the external walls of the CFD model and curtain wall was defined using the smooth-transition method with 20 layers and a transition ratio of 0.242 (Figures 2c, 2e, and 2f). The height of the first element in the boundary layer at the walls of booster fans casings was set at 0.005 m, with 12 layers and a transition ratio of 0.272 (Figures 2e and 2f). The CFD model was meshed using polyhedral cells, with a maximum cell length of 1.07 m and a growth rate of 1.2. Localized mesh sizes were specified at the booster fans and the curtain of 0.05 m and 0.1 m, respectively, with a growth rate of 1.2 (Figures 2c, 2e, and 2f).

MESH CONVERGENCE STUDY

It is essential to perform a mesh independence study to determine the ideal mesh size to optimize computational speed and model accuracy. In this study, three mesh sizes were tested and screened to identify the optimized mesh size. The mesh sizes are coarse, medium, and fine of about 7.6 M, 13.2 M, and 30.1 M cells, respectively. The mesh refinement was defined in the surface meshing step of mesh creation where the maximum size of surface mesh was defined as 1.0 m, 0.8 m, and 0.5 m for coarse, medium, and fine meshes, respectively.

Performing a mesh independence analysis is crucial for identifying the optimal mesh size to enhance computational efficiency and model precision. This study involved testing and evaluating three different mesh sizes: coarse, medium, and fine, comprising approximately 7.6 M, 13.2 M, and 30.1 M cells, respectively. Mesh refinement was applied during the surface meshing stage of ANSYS-Fluent mesh generation, where the maximum surface mesh size was set to 1.0 m, 0.8 m, and 0.5 m for coarse, medium, and fine meshes, respectively.

Figures 3 and 4 illustrate the velocity profiles at stations S6, S7, and S8 within Entry 93 (see Figure 1 for station locations in the mine). These velocity profiles were obtained at distances of 1.67 m (Figure 3) and 4.9 m (Figure 4) above the floor for each station. It is notable that the velocity profiles derived from the medium and fine mesh configurations demonstrate a high degree of consistency, while

the coarse mesh configuration deviates from the others. Consequently, the decision was made to adopt the medium mesh size for conducting CFD modeling of airflow in the study mine.

To validate the established CFD model, a comprehensive analysis was performed by comparing it with data gathered from a mine ventilation survey. Figure 5 illustrates the correlation between the mass-weighted average velocity magnitude as calculated by the CFD model and the actual air velocity measured during the first survey at 33 different locations. The analysis revealed a good correlation, with an R-square value of 0.83, affirming the adequacy of the CFD model's results in comparison to field measurements.

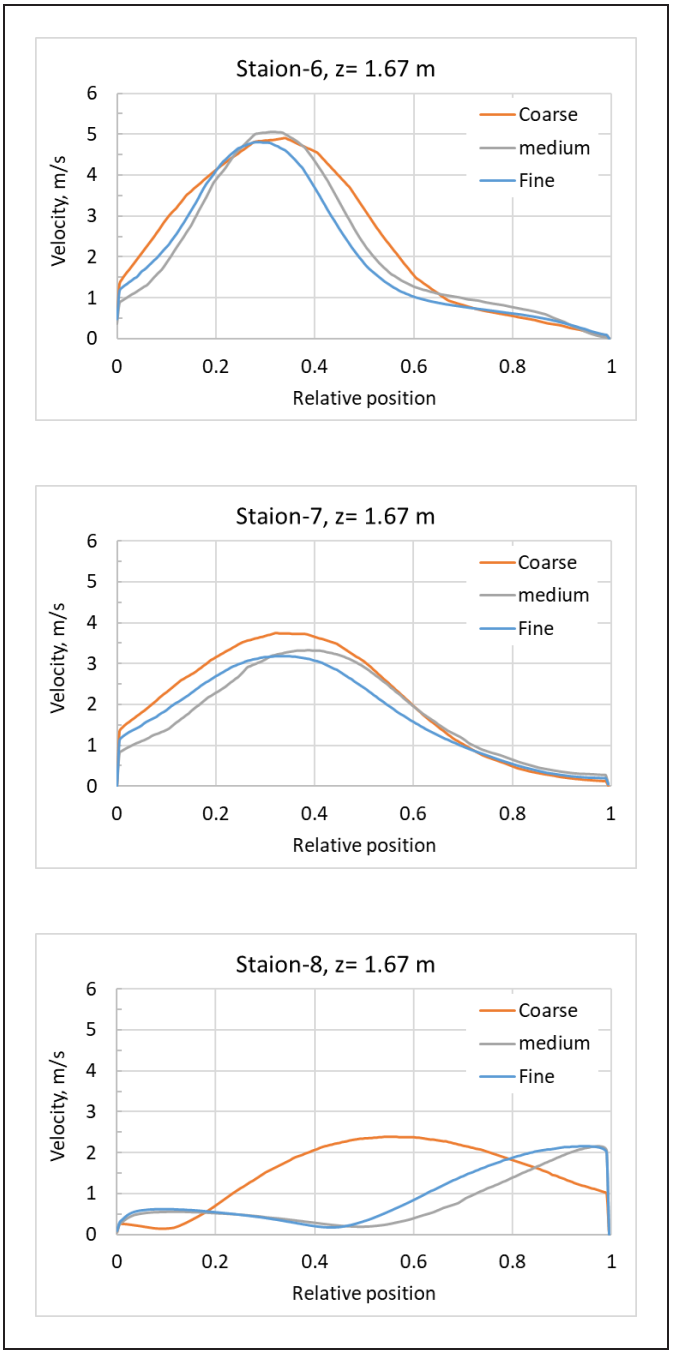

Figure 3. Velocity profiles derived from the CFD model at various stations located at z = 1.67 m, corresponding to entry 93

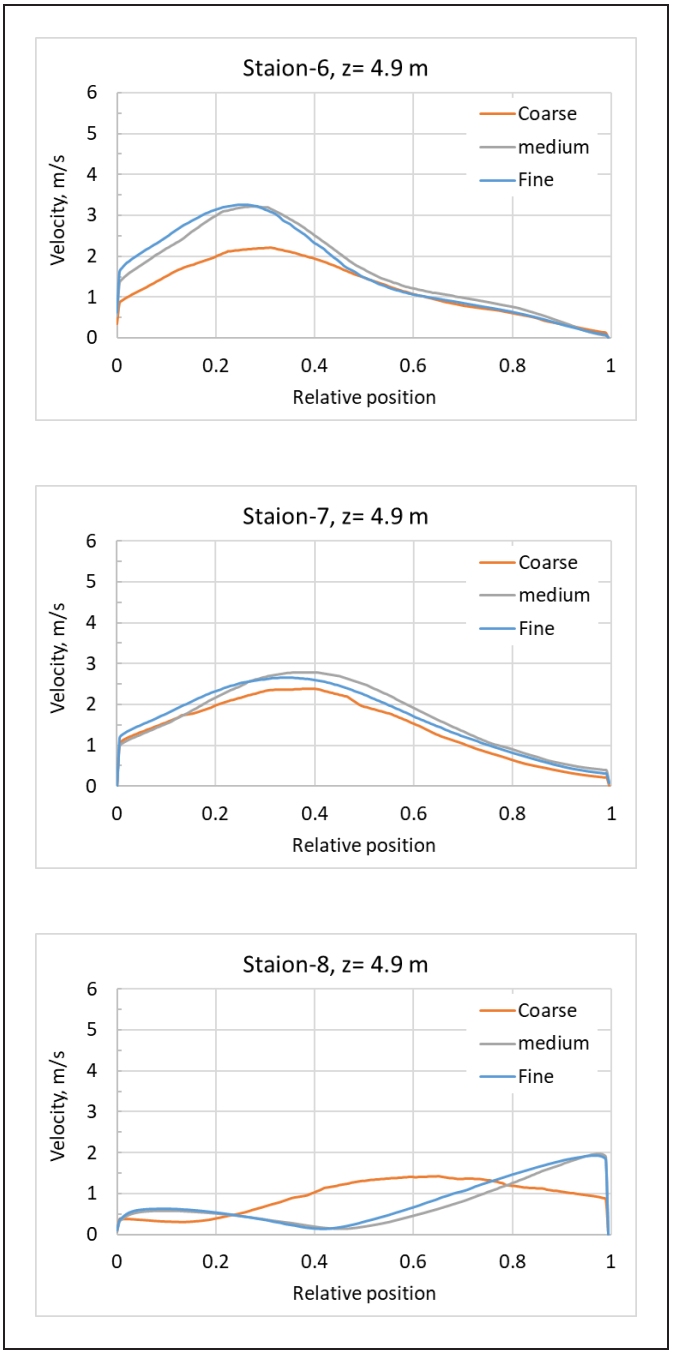

Figure 4. Velocity profiles derived from the CFD model at various stations located at z = 4.9 m, corresponding to entry t93

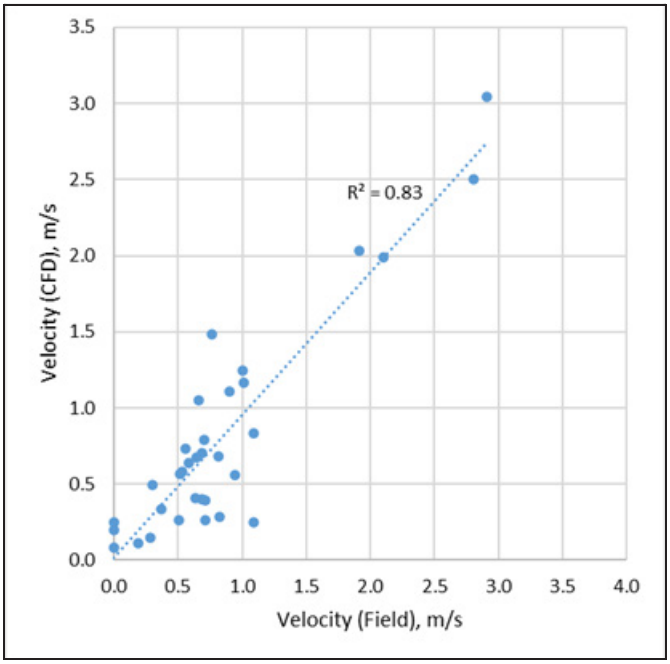

Figure 5. The correlation between the CFD model's average velocity and the measured winter ventilation air velocity

During the ventilation survey, a smoke tube was utilized to visualize the flow patterns in the study mine. Figure 6 presents a representation of the airflow patterns derived from the established CFD model, utilizing input data acquired during the winter ventilation survey. During this survey, airflow directions were determined at 33 stations (refer to Figure 1). Among these 33 stations, the CFD model accurately predicted airflow directions at 24 locations. In five stations where measured air velocities fell below 0.5 m/s, the CFD model estimated reverse airflow directions. In four stations, the CFD model showed air circulations, preventing a direct comparison with field measurements.

Figure 7 illustrates the correlation between the mass-weighted average velocity magnitude as calculated by the CFD model and the actual air velocity measured during the second ventilation survey at 50 different locations. The analysis revealed a lower R-square value of 0.57 in the second ventilation survey. This decrease could be linked to the fact that the mine was actively producing during the second survey. During this period, haul trucks were observed entering through the intake-1 and exiting through the intake-2. With the validation of the model completed, it is now ready for assessing the effects of in-place stone stoppings layouts on the efficiency of face ventilation and air recirculation at crosscuts between exhaust and intake entries.

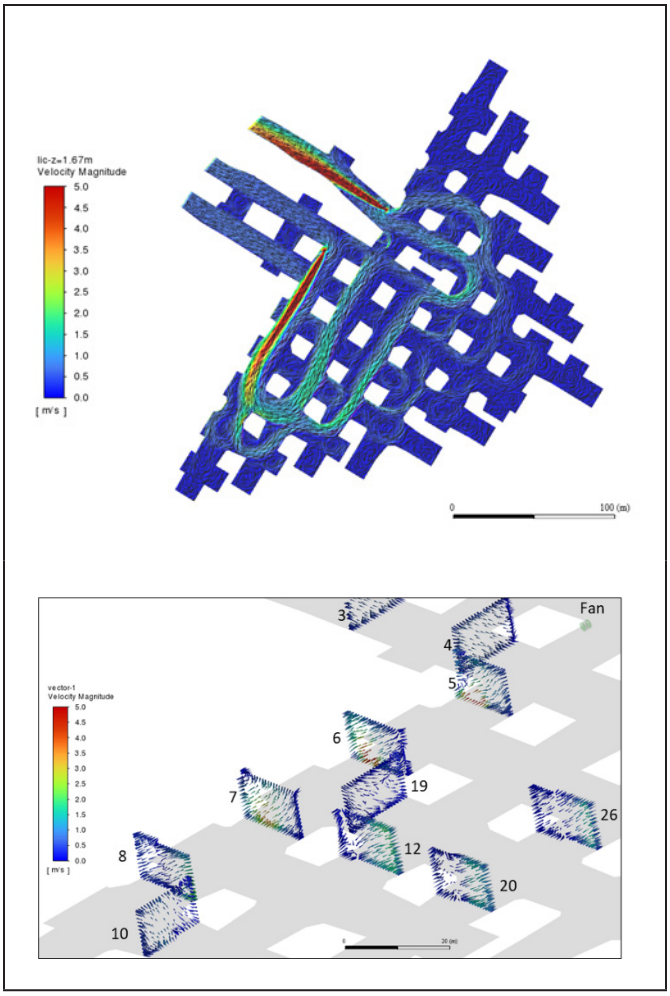

Figure 6. CFD calculations of airflow patterns within the study utilizing winter ventilation survey data as the input for the CFD model

ASSESSMENT OF THE INFLUENCE OF STONE STOPPINGS ON VENTILATION EFFICIENCY

The primary aim of this research paper is to explore how different arrangements of in-place stone stoppings impact the efficiency of face ventilation and the air recirculation at the crosscuts between exhaust and intake entries. Two configurations for these in-place stone stoppings, referred to as Layout-I and Layout-II, were assumed and conducted simulations using the validated CFD models. Layout-I is shown in Figure 8, featuring a shorter in-place stone stopping, while Figure 9 illustrates Layout-II, which incorporates a longer in-place stone stopping.

The model setup closely aligns with the description provided in the previous section, with a few exceptions based on findings from the late spring ventilation survey:

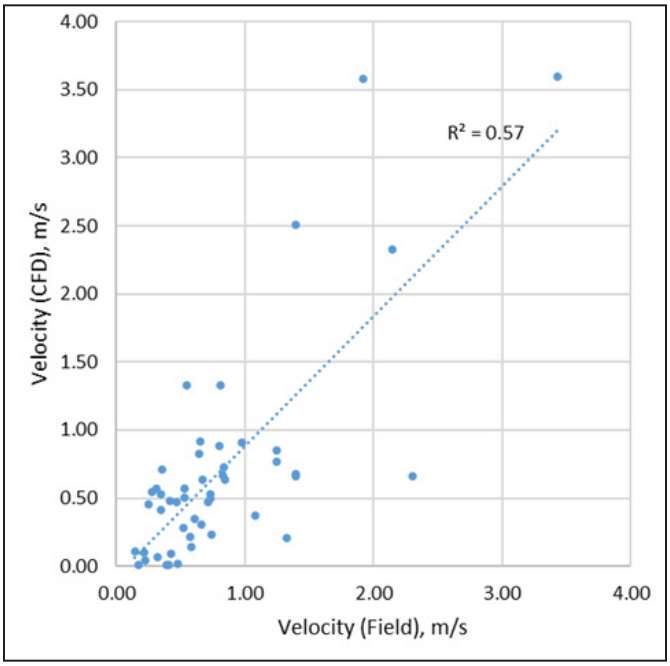

Figure 7. The correlation between the CFD model's average velocity and the measured spring ventilation air velocity

- The new model simulates a larger mined area.
- No air leakage was assumed at the curtain installed in the first crosscut.
- The orientation of the intake fan was adjusted to direct air towards the inby of entry 93, enhancing airflow towards the advanced faces at entries M-59 and M-61 (see Figure 1).
- Pressure boundary conditions were assigned for the model's inlets and outlet.

Figure 8 and Figure 9 show the airflow streamlines computed for Layout-I and Layout-II, respectively. Layout-I and Layout-II exhibit comparable airflow patterns. It is worth mentioning that most of the airflow coming from the Inlet-1 portal moves toward the outlet portal through crosscut (X1), with minimal impact on airflow in other areas. Meanwhile, the airflow at the remaining crosscuts (X2, X3, etc.) originates from the Inlet-2 portal.

Grau et al, 2006 rated mine ventilation system by calculating ventilation efficiency. The ventilation efficiency was defined as the percent of useful ventilation air quantity passing a specific point compared to the total possible air quantity available. Hence, the ventilation efficiency was assessed in this stat seven designated points, labeled as A to G. Table 1 provides the ventilation efficiency results expressed as a percentage of the airflow at each designated face relative to the total inlet airflow of layout-I and layout-II are 191.55 m3/s and 179.74 m3/s, respectively.

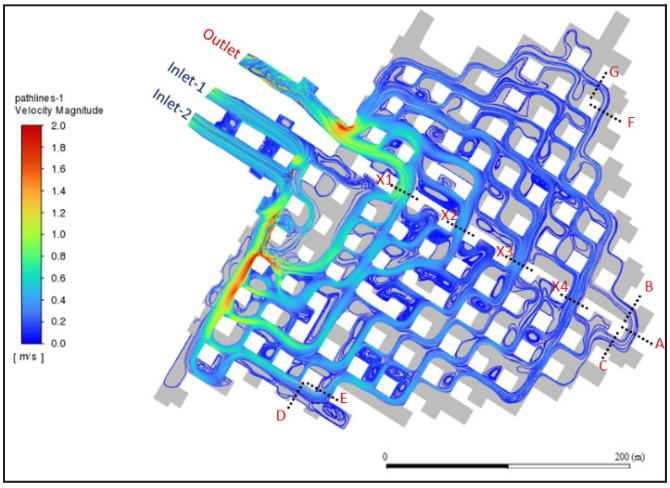

Figure 8. Streamlines of airflow computed for the stone stoppings in Layout-I

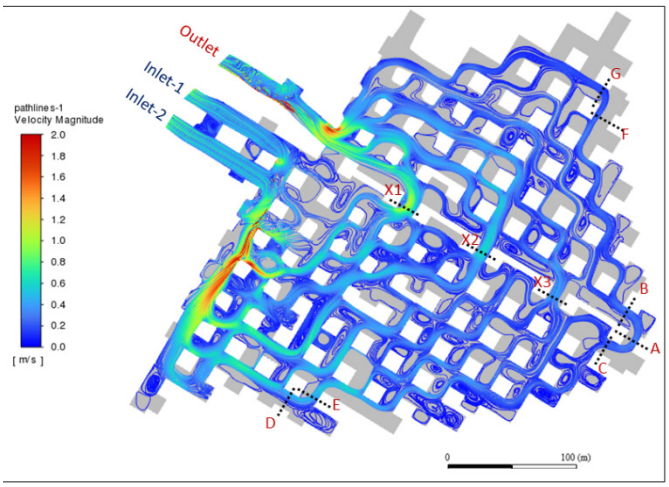

Figure 9. Streamlines of airflow computed for the stone stoppings in Layout-II

Table 1. Airflow and ventilation efficiencies at specific locations within both Layout-I and Layout-II

	Volumetric Flow Rate, m^3/s		Face Ventilation Efficiency, %	
Plane-ID	Layout-I	Layout-II	Layout-I	Layout-II
A	7.6	15.2	4.0	8.4
B	7.7	15.2	4.0	8.4
C	7.6	15.1	4.0	8.4
D	24.7	27.9	12.9	15.5
E	24.7	27.9	12.9	15.5
F	9.6	9.9	5.0	5.5
G	9.6	9.9	5.0	5.5

The findings derived from the CFD models showcased a significant enhancement in ventilation effectiveness at the advanced areas (A, B, and C) within Layout-II, attributed to the increased length of the stone stopping in place.

Table 2. Airflow and percentages of air recirculation at the crosscuts between exhaust and intake entries in both Layout-I and Layout-II.

	Volumetric Flow Rate, m^3/s		Crosscut Air Circulation, %	
Plane-ID	Layout-I	Layout-II	Layout-I	Layout-II
X-1	89.2	83.7	46.6	46.6
X-2	37.9	46.4	19.8	25.8
X-3	33.1	34.3	17.3	19.1
X-4	23.6	n/a	12.3	n/a

This improvement resulted in an efficiency rise from 4% in Layout-I to 8.4% in Layout-II. Nonetheless, a marginal effect on the in-place stopping layouts was noticed at other areas, specifically faces D and F, whereas no impact was observed at faces F and G.

Air recirculation at crosscuts (X1, X2, etc.) has been computed and is presented in Table 2. This computation illustrates the percentage of air recirculation within specific cross-sections compared to the total airflow entering the inlets. Overall, Layout-II showed a higher circulation of air around the outby stoppings (X1 and X2).

SUMMARY

NIOSH researchers conducted two air ventilation surveys in an underground limestone mine in Pennsylvania to validate CFD model for simulating air flow in large opening stone mines. The collaborated mine used a split ventilation system with two intake and one return entrances, featuring 9.15-m height and 15.24-m width entries, and two 1.83-m propeller booster fans. The intake fan directed external air into the mine, while the exhaust fan facilitated air outflow. The first survey involved 60-second anemometer traverses at 33 stations within the mine. Smoke tubes visualized airflow patterns, including stagnant areas. In the second survey, more traverses were conducted, and it was noted ongoing production activities, altered mine boundaries, and reorientation of intake booster fan.

The study utilized ANSYS-Fluent, a widely accepted software tool in underground ventilation engineering, to investigate fluid-flow and heat transfer issues. The study employed a 3D, steady-state, incompressible Navier-Stokes equation solution with Reynolds-averaged (RANS) equations and the k-epsilon turbulence model. Pressure boundary conditions were assigned at the model's inlets and outlet. Booster fans were simulated with constant pressure gradients. The model featured various wall conditions, and gravity was considered. Convergence was achieved within 200–300 iterations. The study recommended a k-epsilon turbulence model approach for large-opening stone mines and a scalable wall function for varied y-plus values. Meshing involved polyhedral cells with specific layer configurations.

Conducting a mesh independence study is crucial to optimize computational speed and model accuracy. This study evaluated three mesh sizes (coarse, medium, and fine) with 7.6 M, 13.2 M, and 30.1 M cells, respectively. Mesh refinement was applied in the surface meshing stage with different surface mesh sizes. Velocity profiles at various stations in a mine were analyzed, leading to the selection of the medium mesh size for CFD modeling due to its consistency.

A CFD model's validity was assessed by comparing it to data from a mine ventilation survey. Results showed good correlation (R-square = 0.83) with 33 winter survey locations. In a spring survey with 50 locations, there was a good correlation (R-square = 0.57).

This research paper investigates the influence of different in-place stone stopping arrangements on face ventilation efficiency and air recirculation at crosscuts between exhaust and intake entries. Two layouts, Layout-I and Layout-II were simulated. Layout-I features shorter stone stoppings, while Layout-II has longer stone stoppings. The study adjusted various factors based on spring ventilation findings, including intake fan orientation and inlet portal mass flow conditions. Airflow patterns were similar for Layout-I and Layout-II, with most airflow from Inlet-1 moving through crosscut (X1). Ventilation efficiency notably improved in Layout-II at advanced faces (A, B, and C), increasing from 4% to 8.4% compared to Layout-I. Other faces (D, E, F, and G) showed no significant impact. Layout-II demonstrated increased air recirculation at outby stoppings.

STUDY LIMITATIONS

In this research, the CFD models were validated using a small mine layout without benching and was not verified to be applied to a larger fully developed mine, mines with different entry and/or pillar sizes, or to one that employs benching. The effect of vehicle movement on airflow was not considered in the model. The primary objective of the modeling exercise was to assess the influence of hypothetical layouts of in-place stone stopping on ventilation efficiency. Despite hypothetical modeling results indicating potential for improved ventilation efficiency, these proposed layouts for in-place stopping have not yet been validated through field testing.

DISCLAIMER

The findings and conclusions in this study are those of the authors and do not necessarily represent the official

position of the National Institute for Occupational Safety and Health (NIOSH), Centers for Disease Control and Prevention (CDC). Mention of any company or product does not constitute endorsement by NIOSH.

KETIV Technologies neither owns nor bears any responsibility for the data collected, presented, and used in this paper for simulation correlation.

REFERENCES

[1] ANSYS (2023). ANSYS Fluent Theory Guide. Release 2023 R1. Canonsburg, PA.

[2] Bhargava, R., Tukkaraja, P., Adhikari, A., Sridharan, S. J. and Vytla, V. V. S. (2021). Airflow characteristic curves for a mature block cave mine. In: Tukkaraja, P. (Ed. Proceedings of the 18th North American Mine Ventilation Symposium. Rapid City, SD, CRC Press.

[3] Gendrue, N., Liu S., Bhattacharyya, S., and Clister R. (2023). An investigation of airflow distributions with booster fan for a large opening mine through field study and CFD modeling. Tunnelling and Underground Space Technology 132 (2023) 104856.

[4] Grau III, R. H. and Krog, R. B. (2009). Ventilating large opening mines. Journal of the Mine Ventilation Society of South Africa, 62, 8–14.

[5] Grau, R. H., Krog, R. B., and Robertson, S. B. (2006). Maximizing the ventilation of large-opening mines. Proceedings of the 11th North American Mine Ventilation Symposium 2006, 53–59. doi.org/10.1201/9781439833391.ch8.

[6] Krog, R.B., Grau, R.H., Mucho, T.P., and Robertson, S.B. (2004). Ventilation Planning Layouts for Large Opening Mines. 2004 SME Annual Meeting, Feb 23–25, Denver, Colorado, preprint 04-187. Littleton, CO: Society for Mining, Metallurgy, and Exploration, Inc., 2004 Feb.

[7] Morla, R., Karekal, S. and Godbole, A. (2021). Transient-flow modelling of DPM dispersion in unventilated dead-end crosscuts and control strategy using curtain. In: Tukkaraja, P. (Ed. Proceedings of the 18th North American Mine Ventilation Symposium. Rapid City, SD, CRC Press.

[8] NMA (2020) Mine Safety & Health Administration's Number of Coal and Non-fuel Mineral Operations in the U.S.

[9] Raj K. V. and Gangrade V. (2023). CFD Modeling of a Large-Opening Stone Mine using COMSOL Multiphysics. Proceedings of the 19th North American Mine Ventilation Symposium (NAMVS 2023, 17–22 June 2023, Rapid City, South Dakota, USA).

[10] Raj, K. V., Bandopadhyay, S. and Ramani, R. V. (2015). Turbulent Models for Pollutant Transport in Openpit Mines under Stable Boundary Layer. Transactions of Society for Mining, Metallurgy, and Exploration, Inc, 338, 476–486.

[11] Watkins E. and Gangrade V. (2022). Optimization of auxiliary fan placement for large-opening underground stone mines. SME Annual Meeting. Salt Lake City, UT.

24-035

Enrichment Feasibility of Tellurium, Gold, and Silver from Copper Tailings

Jose L. Corchado-Albelo
Missouri University of Science & Technology,
Rolla, MO, USA

Lana Alagha
Missouri University of Science & Technology,
Rolla, MO, USA

Fardis Nakhaei
Missouri University of Science & Technology,
Rolla, MO, USA

ABSTRACT

Tellurium (Te), a critical mineral for solar energy technologies, faces supply risk challenges that drive the development of diversified and robust production routes. This research focused on improving Te enrichment from copper tailings (CT) produced from copper porphyry (CP) ores processing, addressing the loss of ~90% of Te minerals to tailings in the flotation process of CP ores. Gravity separation and froth flotation processes were used as possible enrichment routes of Te-bearing minerals (i.e., pyrite) in CT. In the froth flotation process, synergistic combinations of reagents were tested to achieve an acceptable enrichment ratio of Te minerals. Comprehensive characterization analyses showed significant Te enrichment in the flotation concentrates. Tellurium was recovered at 90%, while the grade of Te in the concentrates was 1.4 ppm using a xanthate collector and glycol frother compared to <0.5 ppm in the flotation feed. Findings showed that Te-minerals' enrichment was also feasible in CT using the proposed combined concentrations routes (i.e., gravity separation followed by froth flotation) by looking at Fe, Cu, and S enrichment. This study also highlighted the importance of understanding the deportment of Te minerals in different process streams to develop and optimize efficient enrichment practices.

INTRODUCTION

Tellurium (Te) is a critical mineral in many governmental strategic mineral lists, such as the U.S.A., Canada, United Kingdom, Japan, and India [1–6]. Critical minerals are specific commodities categorized by a government or the private sector because of instability and risks to the supply chain due to trade exposure, supply disruption potential, and economic vulnerability [7–13]. Since the early 2010s, critical minerals have resurged as an issue of interest for research and development because of unstable supply chains, trade exposure, and economic vulnerability of specialized commodities [7,11,13]. The change in the commodity supply chains associated with the transition from fossil fuels to more sustainable energy sources is of increased concern when looking at secure and ethical sourcing/supply of specialized commodities. Consequently, many world governments and private sectors name these elements or commodities as critical minerals [11,14–20]. Tellurium has gained increasing attention in the last decade due to its importance to clean solar energy production, most notably as an essential raw material in cadmium telluride (CdTe) photovoltaic applications. In recent years, the demand for Te has increased as it continues to be incorporated into manifold specialized applications. For example, Te is an additive to metal alloys in glass optical fibers, ceramics as a